Loaded and load-less supergain parasitic end-fire arrays

Alessio Tornese, Antonio Clemente, Christophe Delaveaud

Loaded and load-less supergain parasitic end-fire array

Alessio Tornese*, Antonio Clemente*, Christophe Delaveaud*,
*Univ. Grenoble Alpes, CEA, Leti, F-38000 Grenoble, France
e-mail: {alessio.tornese, antonio.clemente, christophe.delaveaud} @cea.fr

***Abstract*—This paper presents a compact three-bent-dipoles end-fire array with very high realized gain designed at 916 MHz. The optimization consists in feeding the array elements in a proper way to optimize directive properties in a chosen direction of the space, with the constraint of high efficiency. The feeding weights are transformed in complex impedance and used to synthesize a parasitic array. The central element is fed and the external elements loaded with reactive components. The array configuration, featuring three elements equally spaced within a total radiansphere of $kr = 1.44$. A second version with the reactive loads integrated into the array geometry is also designed, by tuning the imaginary parts of the dipole by acting on their vertical length. The two version of the array are matched with a T-match on the active elements. Experimental results on differentially-fed fabricated prototype demonstrate excellent agreement between simulated and measured radiation properties. In the differential mode, the peak realized gain of 8.9 dBi at 910 MHz, and of 8.3 dBi at 911 MHz are measured for the case of parasitic loaded and integrated loads arrays, respectively.**

***Index Terms*—end-fire arrays, supergain, efficiency, compact antennas.**

I. Introduction

The rapid evolution of antenna technology has been driven by the growing demand for high-performance, compact, and cost-effective solutions in various emerging applications such as IoT, Wireless Power Transfer (WPT), (5G), Industry 4.0, and so on. However, these advancements in the case of compact antenna size are constrained by fundamental physical limitations on antenna gain and bandwidth [1]. In recent years, there has been renewed interest in superdirective antennas, which exhibit exceptionally high directivity for their size.

Initially, studies focused on increasing antenna directivity by reducing the overall array dimensions, following Uzkov's principle [2] of increasing directivity as element spacing decreases for end-fire arrays. More recent works have investigated the fundamental limitations of antenna gain for a given geometry and material properties [3] in terms of "lossy characteristic modes" [4] or "multipole-excitations" [5]. Upper bounds for the maximum directivity of end-fire arrays of electrical dipoles and Huygens sources are discussed in [6]. When the directivity limit is reached, the corresponding gain is very low, and this efficiency drop increases as the element spacing vanishes or the total element number in the array increases.

A recent method to calculate losses and optimize gain is proposed in a preliminary study based on the Spherical Wave Expansion (SWE) theory [7], along with a comparison of directivity and gain optimization for a three-element end-fire array based on Huygens sources and bent dipoles [8]. The maximum directivity attained for Huygens-sources-based end-fire arrays is much higher than the one for the electrical-dipoles case, aligned with [6]. However when gain is targeted the two arrays presents very similar values of maximum gain, and considering the complexity of design and feeding of the structure, electrical dipoles remain the more convenient choice for designing compact end-fire arrays.

Experimental realizations of compact and efficient superdirective antennas can be found in [9], where an optimal shape synthesis based on surface currents and modal analysis is used to design an antenna with 6.7 dBi of intrinsic gain and a $kr = 0.9$. In a study [10], a clever design based on the "multipole-excitation" approach achieves a measured realized gain of 6.3 dBi at $kr = 1$. Additionally, [11] reports an intrinsic gain of 8.6 dBi for a three-element end-fire ($kr = 1.4$) array synthesized based on the array factor theory.

This paper presents a practical demonstration of the optimization performed using an SWE-based analytical model for gain maximization, yielding to a higher realized gain of 8.9 dBi for a similar design as the one presented in [11], matched at the desired frequency. Moreover, the use of a balun is bypassed with a differential feeding, eliminating an external source of losses. To achieve the impedance match at the desired frequency of 916 MHz, in the same $kr = 1.44$ condition, a printed T-match is realized. The optimal impedance profile of each array element is obtained by parasitically loading the two external elements while feeding the central one. The difference with previous optimizations is that the loads are calculated prioritizing purely reactive values. A second version of the design is proposed as load-less and still optimized for maximum gain in the end-fire direction. The uncertainty introduced by tolerances and the narrower bandwidth effect attributed to lumped elements is eliminated by directly integrating loads into the element's geometry. Tuning the dipole's impedance can be done by adjusting their lengths. These two designs are fabricated, and the prototype's radiation characteristics are measured in an anechoic chamber.

The paper is organized as follows: Section II discusses the synthesis of supergain end-fire arrays using SWE theory, Section III presents the design of the three-bent-dipoles end-fire arrays with the integrated T-match for the parasitic loaded version and the load-less version. Furthermore, in Section IV, results from the measured prototypes are reported, and

conclusions are drawn.

II. Synthesis of Supergain End-Fire Arrays

A. Optimal coefficients extraction

Let us assume an end-fire array of P radiating sources uniformly spaced by d. The reference system is chosen in spherical coordinates θ, ϕ such that the end-fire radiation chosen is identified with $(\theta_0 = 0, \phi_0 = 90)$. The active pattern of each array element $E_p(\theta, \phi)$ can be calculated through electromagnetic simulations, as well as the radiation efficiency associated with each radiator $\eta_{rad,p}$. The objective is to define the element feed in terms of complex weighting coefficients α_p that optimize directivity in the direction θ_0, ϕ_0, with the additional constraint of keeping high the total array efficiency. To this purpose, an optimization method based on the SWE theory is used. The first step consists of expressing the $E_p(\theta, \phi)$ in terms of spherical coefficients $Q_{smn,p}$. These coefficients allows the reconstruction of the original field as

$$E_p(\theta, \phi) = \frac{k}{\sqrt{\eta_0}} \sum_{smn} Q_{smn,p} \cdot K_{smn}(\theta, \phi), \tag{1}$$

with k the wavenumber, η_0 the vacuum impedance, and $K_{smn}(\theta, \phi)$ the spherical wave functions as defined in [6]. From the SWE theory the optimal modal distribution for maximum directivity in the desired direction is given by the spherical coefficients $Q^{opt}_{smn} = [K_{smn}(\theta_0, \phi_0)]^*$ [6]. Then, by following the procedure in [6] and the introduction of the losses as indicated in [12] it is possible to calculate the optimal weighting coefficients for maximum gain as

$$\alpha_p = \sum_{smn} Q^{\dagger}_{smn,p} Q^{opt}_{smn}, \tag{2}$$

B. Optimal loads

The coefficients α_p of (2) are proportional in amplitude and phase to the values of the voltage/currents that must be established on the array elements to satisfy the optimization process. The full-driven configuration can be substituted feeding a central active elements and the remaining excited by coupling. To control the currents running on the passive elements their impedance can be tuned, as suggested in [13], loading the antenna element with an impedance value $Z_{L,p}$. These impedance values depends on the complex coefficients derived from optimization as well as the impedance matrix of the entire array. The extraction of the desired impedance loads hinges on the scattering parameters, and this process is elaborated in detail in [13]. The return loss for each element, as a function of the scattering parameters and the imposed power waves, can be expressed as

$$\Gamma_p = \frac{\alpha_p}{\sum_{i=1}^{P} S_{pi} \alpha_i}, \tag{3}$$

The parasitic loads, which influence the radiation by means of coupling in a similar manner, are given by solving

$$Z_{L,p} = Z_0 \frac{1 + \Gamma_p}{1 - \Gamma_p}, \tag{4}$$

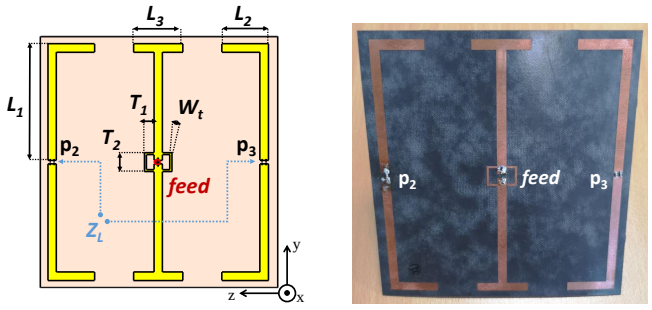

(a) (b)

Fig. 1. Parasitic loaded end-fire array: the simulated geometry with labeled dimensions (a), and the photograph of the fabricated prototype (b).

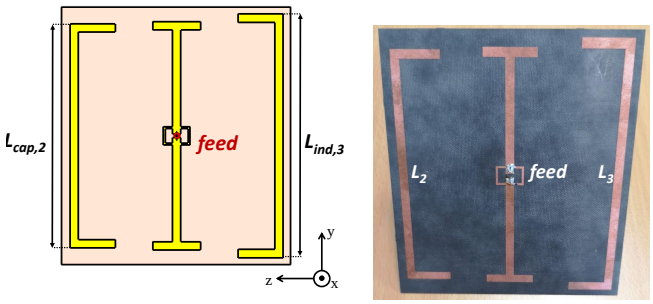

(a) (b)

Fig. 2. Load-less version of the designed end-fire array: the simulated geometry with labeled dimensions (a), and the photograph of the fabricated prototype (b).

where Z_0 is the reference impedance (50 Ω). Parasitic loading simplifies the design process by modifying the impedance profile of antennas using lumped elements. To minimize losses, it is preferable to employ purely reactive loads, thereby avoiding the utilization of resistors [14], [15].

III. Design of the Three-Elements Bent-Dipoles End-Fire Array

A. The array geometry

The design proposed is a three-dipoles end-fire array spaced by $d = 0.15\lambda$. The external elements are bent dipoles placed symmetrically to the origin, thus reducing the total kr for a fixed d. The vertical arms of the bent dipole have a length $L_1 = 0.165\lambda$, i.e. a vertical size reduction of 32% (w.r.t. the $\lambda/2$ version), and the horizontal arm $L_2 = 0.06\lambda$. The center element has the same vertical arm of length L_1, and an horizontal miscrostrip line acting as a top loading of length $L_3 = 0.065\lambda$. The microstrip lines of width $W_m = 3.5mm$ are made of copper ($\sigma = 5.8e9$) and the dielectric substrate is Rogers RT5880 ($\epsilon_r = 2.2$ and $tan\delta = 0.0009$) with thickness of $0.78mm$. The overall array size is $kr = 1.44$. The geometry of the proposed design is illustrated in Fig. 1a.

The array is optimized according to the synthesis procedure described in Section II. The data resulting from the electromagnetic simulations are used to calculated the optimal feeding α_p coefficients (2). Then, with the simulated S-parameters and the optimal impedance loads are extracted

according to 4. These loads are $Z_{L,2} = 24$ pF and $Z_{L,3} = 2.2$ nH on port 2 and 3 respectively.

B. Impedance matching

When the final geometry (Fig. 1a) and loads are set, antenna impedance matching to the reference impedance is the next step. A T-match is used, since it can be easily integrated in the planar structure and does not use additional components. According to antenna matching techniques, the input impedance of a dipole can be fixed to the desired impedance by feeding a transmission line (TL) with a specific geometry closely spaced to the antenna element, and connected to it. By adjusting the TL's length T_2 and width W_t, the impedance can be controlled. The extremities of the TL are then connected to the arm of the dipole at a distance $T_2/2$ from the center. The distance between the TL and the dipole T_1 is another key parameter to adjust the impedance. In our case, to symmetrically connects the two arms of the active elements, a mirrored T-match is designed as shown in Fig. 1. In order to keep a balance, the feeding point is kept on the central dipole, and the two symmetrical T-match are short-circuited. The parametric simulations of the T-match parameters show optimal results for $T_2 = 0.012\lambda$, $T_1 = 0.01\lambda$, and $W_t = 1$ mm dimensions. The simulated results will be directly shown with the experimental one in the next Section IV.

C. Unloaded version

The loads effect is to redistribute the power, accounting for mutual coupling, among the array elements to obtain a specific current and pattern. The optimal loads $Z_{L,2}$ and $Z_{L,3}$ previously obtained modify the imaginary part of the external dipoles according to their capacitive or inductive values. On this basis, by keeping the same array structure (elements geometry, spacing, etc...) the inductive and capacitive behavior demanded by the optimization are obtained by acting only on the vertical dipole's length. The length of the vertical arms represent the radiating part of the electrical path of the current on the element. Increasing the length of the dipole antenna corresponds to an augmentation of the imaginary part of the impedance, thereby enhancing its inductive characteristics. Similarly, reducing the length of the dipole increase its capacitive nature. In a nutshell this concept was the one used by the Yagi-Uda antennas [16], with the difference that in this case very compact dimensions and an element spacing way shorter than $\lambda/4$ is employed. With these concepts in hand, the lengths of the two dipoles are modified as $L_{cap,2} = 0.98$ L_1 and $L_{ind,3} = 1.07$ L_1. The geometry of the optimized load-less design is illustrated in Fig. 2a. The electromagnetic simulations report a slightly lower level of gain with respect to the previous case using optimal loading. However, the beam is shaped in the same direction and a good impedance matching at the desired frequency is obtained, resulting in a high realized gain. All these results are detailed and compared to the measurements in the next Section IV.

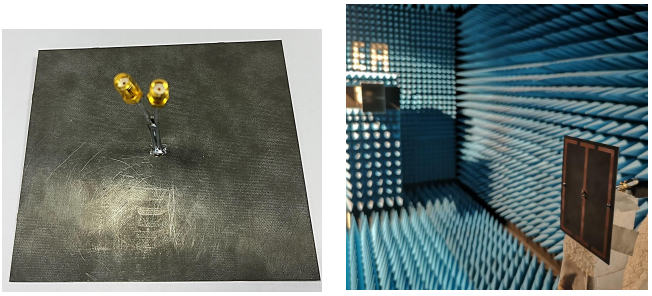

(a) (b)

Fig. 3. Photographs: bottom view of the prototype where two coaxial cables are soldered (a) and the anechoic chamber for radiation properties measurement (b).

IV. Prototype and Measurements

A. Differential-feeding

In principle, the differential feeding consists in applying signals of same amplitude and opposite phase to the two arms in the case of a dipole antenna. In this way, when summing up the field generated by the currents excited by each of the two opposite signals, the common mode is canceled out. The component resulting from the combination of the two excitation is attributed to the differential mode. In the presented design the differential feeding is obtained by using two coaxial cables, each one connected to one arm of the central dipole. This step is simulated in CST, to ensure that the configuration works well and can excite the desired modes. Then, two coaxial cables are designed and positioned perpendicular to the bottom part of the substrate of the array (see Fig. 3a). Then, waveguide ports are applied to each cable and the structure is simulated. The results of the two ports can be combined in CST post-processing function, choosing a differential port and connect to the two waveguide port. To "deembed" the S-parameter values, the cables are simulated with the terminals short-circuited, and closed on a matched load (50 Ω). The results are then used to extract the correct S-parameters of the structure removing the effect of the coaxial cables, with a post-processing step performed in MATLAB. These results are presented and compared with the measured values in the following paragraph.

B. Simulated and experimental results

The design previously introduced are fabricated and characterized at CEA's facilities in Grenoble (Fig. 3b). The scattering parameters are measured using the Vector Network Analyzer (VNA). The S_{11} could not be directly measured since a differential feeding is employed. Then, the S-matrix from the 2-ports network is extracted and post-processed to remove the cables effects and extract the differential mode S_{11}. The results are illustrated in Fig. 4, and a very good agreements is observed between the simulations and the measurements. For the parasitic loaded array the impedance match is attained at 911 MHz, with a minima of the return loss of -12 dB. The

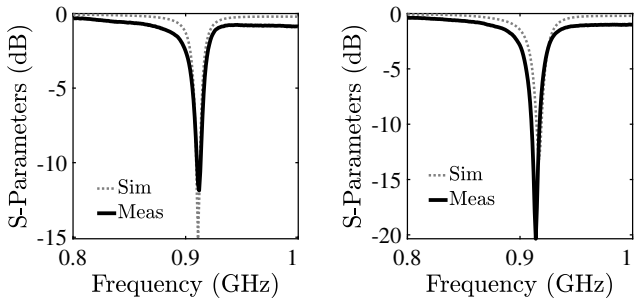

Fig. 4. Comparison between simulated and measured data for the impedance matching S_{11} of the parastic loaded array (a) and the load-less version (b).

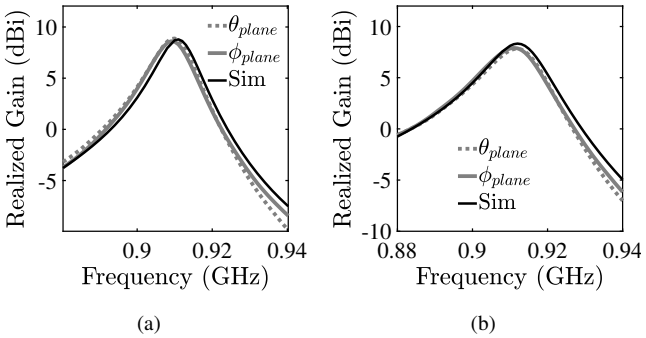

Fig. 5. Comparison of the simulated and measured realized gain around the central frequency of 916 MHz for the parasitic loaded array (a) and the load-less version (b).

load-less version show even better agreement with simulations, where at 912 MHz a minima of -20 dB is measured.

For the measurements of the antenna radiation properties in anechoic chamber (Fig. 3b) one of the two ports of the antenna is fed by using an RF-optic transducer (non-metallic cable), while the other is terminated on a matched load. Two planes are measured: "θ" and "ϕ". In both cases the co-polarization

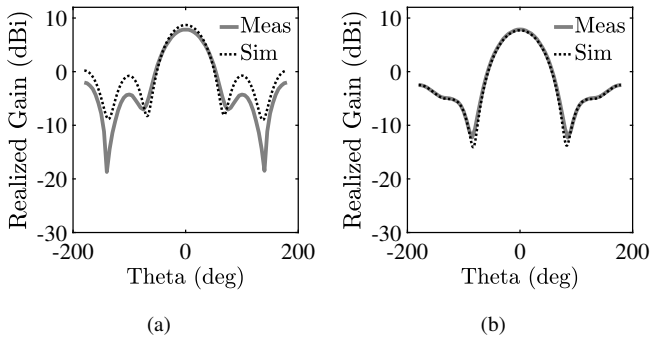

Fig. 6. Comparison of the simulated and measured realized-gain 3D-pattern (θ component) for $\phi_0 = 0$ for the parasitic loaded array (a) and the load-less version (b). Note that in each case the measured pattern is extracted at the frequency point where the maximum is found.

is acquired and the differential realized gain is reconstructed by combined the data acquired by the two port, according to [17]. The values obtained are in very good agreement with the simulations. The parasitic loaded array shows a small frequency shift and presents a peak realized gain of 8.9 dBi at 916 MHz simulated and at 911 MHz measured, as reported in Fig. 5b. A small frequency shift is observed, due to the effect of small fabrication imperfection, or mainly tolerances of the soldered loads. At the frequencies where the maximum are observed the realized gain pattern are extracted for $\phi_0 = 0$ in the simulated and measured case, as illustrated in Fig. 6a. A generally good agreement is found, and levels of secondary lobes are observed to be lower in measurements.

The load-less version of the design presents a peak realized gain of 8.3 dBi simulated at 916 MHz, and the measured peak of 8.2 dBi is found at 912 MHz, as reported in Fig. 5b. Similarly, at the frequency of the maxima for the simulated and measured cases the realized gain patterns ($\phi_0 = 0$) are extracted and compared. Results of Fig. 6b show an excellent agreement. The slightly different level of realized gain registered in frequency in the two cases (Fig. 5) may be due to a slight misalignment between the measured antenna and the horn in the anechoic chamber, or simply the uncertainty of the measurement itself.

V. Discussion and conclusion

This paper introduces a straightforward yet highly efficient design of two compact end-fire arrays based on dipole radiators. Electromagnetic simulations and experimental validations report a high realized gain > 8 dBi for a $kr = 1.44$. Notably, these realizations are deemed to exhibit supergain characteristics, as per the conventional constraints established in the literature by Harrington [1]. The gain optimization is based on the SWE theory, as in [12] where a preliminary work discusses the directivity optimization conditioned with the information of efficiency.

Furthermore, this work introduces two novel elements to the field. First, the impedance matching of the compact array is addressed, aiming to attain a maximum realized gain. This objective is realized through the design of a custom T-match network, meticulously tailored to adjust the impedance characteristics of the array to 50 Ohms. Second, the methodology incorporates a differential feeding approach, obviating the need for a balun and thereby avoiding potential additional losses.

The optimization is based on the synthesis of optimal loads to tune the impedance profile of the parasitic coupled array, where only the central element is fed, and the external are loaded with specific values of impedances. As an interesting alternative, a second version is realized by removing the loads, replaced by adjusting the dipole's length to mimic the effect of the reactive loads. Employing lumped elements could represent a source of uncertainty and error, as well as potentially introduce small value of resistance. Comparing these two approaches, the traditionally parasitic loaded array exhibits higher levels of realized gain, reaching up to 8.9

dBi, in contrast to the 8.2 dBi measured for the load-less configuration. However, it is noteworthy that the load-less configuration demonstrates excellent congruence between simulated and measured radiation properties, especially for gain pattern, including side-lobes level, highlighting the potential to optimize the array without the need for lumped elements.

The phenomenon of supergain appears to be intricately linked to the impedance profiles of the array elements, suggesting that it is conceivable to tailor an optimal set of elements that, when coupled together, efficiently excite superdirective modes within the structure.

ACKNOWLEDGMENT

The authors would like to thank Dr. HDR P. Pouliguen and Dr. P. Potier for their useful suggestions and comments on the work presented in this manuscript. This work is partially supported by the DGA (Direction générale de l'armement) and by the French National Research Agency through the project "COMET5G" under the grant ANR-19-CE24-0010-01.

REFERENCES

[1] R. Harrington, "On the gain and beamwidth of directional antennas," vol. 6, no. 3, pp. 219–225. [Online]. Available: http://ieeexplore.ieee.org/document/1144605/

[2] A. I. Uzkov, "An approach to the problem of optimum directive antenna design," pp. 35–38.

[3] M. Gustafsson and M. Capek, "Maximum gain, effective area, and directivity," vol. 67, no. 8, pp. 5282–5293. [Online]. Available: http://arxiv.org/abs/1812.07058

[4] M. Capek and L. Jelinek, "Fundamental bound on maximum antenna gain as a sum of characteristic modes," in *2023 17th European Conference on Antennas and Propagation (EuCAP)*, 2023, pp. 1–4.

[5] R. W. Ziolkowski, "Mixtures of multipoles—should they be in your em toolbox?" *IEEE Open Journal of Antennas and Propagation*, vol. 3, pp. 154–188, 2022.

[6] A. Debard, A. Clemente, A. Tornese, and C. Delaveaud, "On the maximum end-fire directivity of compact antenna arrays based on electrical dipoles and huygens sources," vol. 71, no. 1, pp. 299–308. [Online]. Available: https://ieeexplore.ieee.org/document/9944623/

[7] A. Tornese, A. Clemente, and C. Delaveaud, "A new method for end-fire array gain optimization using spherical wave expansion," in *2022 IEEE International Symposium on Antennas and Propagation and USNC-URSI Radio Science Meeting (AP-S/URSI)*. IEEE, pp. 1232–1233. [Online]. Available: https://ieeexplore.ieee.org/document/9887101/

[8] ——, "Compact end-fire arrays: from theory to directivity and gain maximization," in *2023 17th European Conference on Antennas and Propagation (EuCAP)*, 2023, pp. 1–5.

[9] R. Li, D. McNamara, G. Wei, and J. Li, "Increasing radiation efficiency using antenna shape optimization approach," *IEEE Antennas and Wireless Propagation Letters*, vol. 17, no. 3, pp. 393–396, 2018.

[10] T. Shi, M.-C. Tang, R. Chai, and R. W. Ziolkowski, "Multipole-based electrically small unidirectional antenna with exceptionally high realized gain," *IEEE Transactions on Antennas and Propagation*, vol. 70, no. 7, pp. 5288–5301, 2022.

[11] A. Debard, A. Clemente, L. Batel, and C. Delaveaud, "Experimental demonstration of a supergain three-dipole-end-fire-array," in *2022 16th European Conference on Antennas and Propagation (EuCAP)*. IEEE, pp. 1–4. [Online]. Available: https://ieeexplore.ieee.org/document/9769218/

[12] A. Tornese, A. Clemente, and C. Delaveaud, "A new method for gain prediction of superdirective end-fire arrays," in *2022 16th European Conference on Antennas and Propagation (EuCAP)*. IEEE, pp. 1–4. [Online]. Available: https://ieeexplore.ieee.org/document/9769630/

[13] A. E. S. A. G. Z. E. N. F. F. Y. A. E. A. F. T. T. M. M. Thevenot, C. Menudier, "Synthesis of antenna arrays and parasitic antenna arrays with mutual couplings," *International Journal of Antennas and Propagation*, pp. 1–22, 2012. [Online]. Available: https://www.hindawi.com/journals/ijap/2012/309728/references

[14] R. Haviland, "Supergain antennas: possibilities and problems," vol. 37, no. 4, pp. 13–26. [Online]. Available: http://ieeexplore.ieee.org/document/414725/

[15] M. T. Ivrlač and J. A. Nossek, "High-efficiency super-gain antenna arrays," in *2010 International ITG Workshop on Smart Antennas (WSA)*, 2010, pp. 369–374.

[16] G. Thiele, "Analysis of yagi-uda-type antennas," *IEEE Transactions on Antennas and Propagation*, vol. 17, no. 1, pp. 24–31, 1969.

[17] R. Bourtoutian, C. Delaveaud, and S. Toutain, "Differential antenna design and characterization," in *2009 3rd European Conference on Antennas and Propagation*, 2009, pp. 2398–2402.